Proceedings of the ASME 2010 3rd Joint US-European Fluids Engineering Summer Meeting and 8th International Conference on Nanochannels, Microchannels, and Minichannels
FEDSM-ICNMM2010
August 1-5, 2010, Montreal, Canada

FEDSM-ICNMM2010-30639

SEMI-ANALYTICAL DETERMINATION OF THE ONSET CONDITIONS OF THERMOACOUSTIC ENGINES

Matthieu Guedra
Laboratoire d'Acoustique
Université du Maine
Avenue Olivier Messiaen
72085 Le Mans Cedex 9
FRANCE
Email: matthieu.guedra.etu@univ-lemans.fr

Guillaume Penelet
Pierrick Lotton
Laboratoire d'Acoustique
Université du Maine
Avenue Olivier Messiaen
72085 Le Mans Cedex 9
FRANCE

ABSTRACT

Several analytical or numerical models available in the litterature allow to predict the onset of thermoacoustic engines [5, 6, 11]. However, most of these models rely on strong assumptions concerning for instance the stack geometry or the shape of the temperature field in the thermoacoustic core. The purpose of the work presented here is to put forward a new method allowing the prediction of the onset of the thermoacoustic instability while being exempted from a certain number of these assumptions. This method consists in measuring the transfer matrix of the thermoacoustic core by means of an appropriate experimental setup developed in our laboratory. The results are then introduced into an analytical modeling leading to the prediction of the onset conditions (in terms of heating power supply and acoustic frequency) of the thermoacoustic instability in an engine of specified geometry (straight duct or closed loop, coupled or not with an acoustic load like a secondary resonator or an electrodynamic alternator). The results of measurements will be presented, and the predictions of the onset obtained from these measurements will be compared with those actually observed in a standing-wave thermoacoustic engine.

INTRODUCTION

The thermoacoustic amplification process results from the thermal interaction between an oscillating fluid and a solid surface exposed to a temperature gradient. This interaction is responsible for acoustic work generation and hydrodynamic heat transfer. Thermoacoustic engines are acoustic resonators which use and amplify this effect in a stack of solid plates to transform heat into sound wave. When a critical temperature gradient is held along the stack (i.e. when the onset power of heating is reached), a self-sustained acoustic wave, called "thermoacoustic instability", is generated in the resonator.

For now about twenty years, the optimisation of thermoacoustic engines led to increasing efficiency. Among the most efficient prototypes, one can quote the ThermoAcoustic-Stirling Heat Engine developped by G. Swift and S. Backhaus which provides $700W$ of acoustic power with an efficiency of 30% [7]. Such kind of engine may be coupled for instance with a linear alternator for the production of electricity [10] with good efficiency thanks to the advantageous properties that offers the thermoacoustic conversion (i.e. simplicity, reliability, low cost, environmental protection,...).

The design and the optimisation of most of the existing prototypes are done from one part with the help of available softwares based on the linear thermoacoustic theory, and from the other part in a semi-empirical way. The saturation of the acoustic wave amplitude beyond the onset results from many nonlinear effects

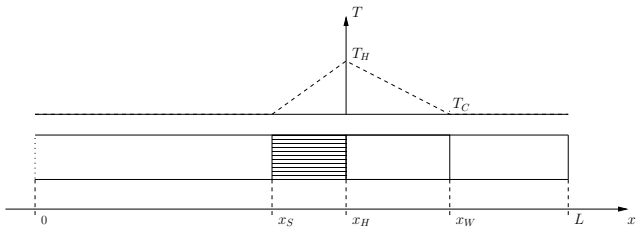

FIGURE 1. DRAWING OF A STANDING-WAVE ENGINE.

which are still poorly understood to date. Concerning the prediction of the onset conditions, several analytical or numerical models [5, 6, 11] are available but these models necessarily rely on strong assumptions concerning the stack geometry or the shape of the temperature field along the thermoacoustic core. More precisely, the stack geometries generally considered for modeling are often simple (network of parallel plates or pores with square or cylindrical section [2,3]) compared to those used in actual engines (wire mesh, "pin-array stacks",...). Concerning the temperature field in the thermoacoustic core, it is often supposed to be linear (in accordance with Fig. 1) and uniform through the resonator's cross section, while the actual temperature distribution is more complicated.

The purpose of the work presented in this document is to put forward a new approach for the precise prediction of the onset conditions of thermoacoustic engines, which is based on the preliminary measurement of the transfer matrix of a thermoacoustic core, without any assumptions on its thermophysical or geometrical properties.

In a first part, the general theory which allows to derive the onset conditions of an engine from this transfer matrix is exposed. In particular, it is shown that the formalism can be used to describe easily the onset for a large number of configurations of engines. The second part describes the experimental setup used to obtain the transfer matrix of a thermoacoustic core on a frequency range from 50 to 200 Hz and for several heating power supplies Q_H. The results are analyzed and compared with those obtained theoretically. The third part presents some preliminary predictions of the onset conditions prediction in the case of a standing-wave thermoacoustic engine. These results are compared with those actually observed in experiments.

1 ANALYTICAL FORMULATION OF THE ONSET CONDITIONS OF THERMOACOUSTIC ENGINES

1.1 Standing-wave engine

A schematic drawing of a thermoacoustic standing-wave engine is shown in Fig. 1. It is made up of an acoustic resonator (straight tube) in which the thermoacoustic core is enclosed. This thermoacoustic core includes the stack situated between $[x_s, x_H]$, and the heterogeneously heated part of the waveguide situated between $[x_H, x_w]$ and named the passive part of the thermoacoustic core.

The assumption of a harmonic plane wave of angular frequency ω allows to write the acoustic pressure as

$$p(x,t) = \Re(\widetilde{p}(x)e^{-j\omega t}), \tag{1}$$

where $\widetilde{p}(x)$ is the complex amplitude of the acoustic pressure at position x and $\Re()$ denotes the real part of a complex number. In the same way, the acoustic volume velocity $u(x,t)$ is expressed in an equivalent form. The use of the transfer matrix formalism allows to connect the acoustic pressure and volume velocity at each point of the engine as :

$$\begin{pmatrix} \widetilde{p}(L) \\ \widetilde{u}(L) \end{pmatrix} = T_2 \times \begin{pmatrix} \widetilde{p}(x_w) \\ \widetilde{u}(x_w) \end{pmatrix}, \tag{2}$$

$$\begin{pmatrix} \widetilde{p}(x_w) \\ \widetilde{u}(x_w) \end{pmatrix} = T_w \times \begin{pmatrix} \widetilde{p}(x_H) \\ \widetilde{u}(x_H) \end{pmatrix}, \tag{3}$$

$$\begin{pmatrix} \widetilde{p}(x_H) \\ \widetilde{u}(x_H) \end{pmatrix} = T_s \times \begin{pmatrix} \widetilde{p}(x_s) \\ \widetilde{u}(x_s) \end{pmatrix}, \tag{4}$$

$$\begin{pmatrix} \widetilde{p}(x_s) \\ \widetilde{u}(x_s) \end{pmatrix} = T_1 \times \begin{pmatrix} \widetilde{p}(0) \\ \widetilde{u}(0) \end{pmatrix}, \tag{5}$$

where T_1, T_w, T_s and T_2 are the transfer matrices of each part of the engine (Fig. 1).

The transfer matrices T_1 and T_2, describing the propagation of plane waves in the wave-guide sections at room temperature ($x \in [0, x_s] \cup [x_w, L]$) are obtained from the expression of the transfer matrix between two points x_A and x_B of a waveguide

$$T = \begin{pmatrix} \cos[k_w(x_B - x_A)] & \frac{ik_0 Z_w}{k_w} \sin[k_w(x_B - x_A)] \\ \frac{ik_w}{k_0 Z_w} \sin[k_w(x_B - x_A)] & \cos[k_w(x_B - x_A)] \end{pmatrix}, \tag{6}$$

where $k_0 = \frac{\omega}{c_0}$ is the acoustic wave number without losses and c_0 is the adiabatic sound velocity. The complex wave number

$$k_w = k_0 \sqrt{\frac{1 + (\gamma - 1) f_\kappa}{1 - f_\nu}}, \tag{7}$$

takes into account the viscous and thermal losses in the vicinity of the resonator's walls and depends on the functions f_ν and f_κ which characterize viscous and thermal coupling between the oscillating fluid and the walls (γ is the specific heat ratio of the fluid, and the analytical expressions of f_ν and f_κ can be found elsewhere [3]). In Eq. (6), the coefficient $Z_w = \frac{\rho_0 c_0}{(1 - f_\nu) S_w}$ is a complex impedance, where ρ_0 and S_w represent the mean density of fluid and the tube cross section, respectively.

T_s and T_w are the transfer matrices of the stack and the passive part of the thermoacoustic core. They can be analytically written, either as an infinite sequence of integral operators [11], or in a simpler approximated form based on strongest assumptions [9]. The first form is more satisfying because it is an exact solution of the linear thermoacoustic propagation equation, though it can only be solved in a numerical way by truncating the infinite sequence. Note that the analytical expressions of the matrices T_s and T_w can only be obtained from making some assumptions concerning the geometry of the pores or the shape of the temperature field.
In this paper, the analytical expressions of T_s and T_w are supposed to be known, either from theory or from experiments. The equations (2) to (5), associated with the continuity of acoustic pressure and volume velocity, lead to

$$\begin{pmatrix} \widetilde{p}(L) \\ \widetilde{u}(L) \end{pmatrix} = T_{tot} \times \begin{pmatrix} \widetilde{p}(0) \\ \widetilde{u}(0) \end{pmatrix} = \begin{pmatrix} T_{pp} & T_{pu} \\ T_{up} & T_{uu} \end{pmatrix} \times \begin{pmatrix} \widetilde{p}(0) \\ \widetilde{u}(0) \end{pmatrix}, \tag{8}$$

where T_{tot} is the global transfer matrix defined as

$$T_{tot} = T_2 \times T_w \times T_s \times T_1. \tag{9}$$

Then, the use of appropriate boundary conditions at $x = 0$ and $x = L$ allows to establish the onset conditions of the engine. For example, in the case of the engine shown in Fig. 1, the open end at $x = 0$ corresponds to an acoustic pressure $\widetilde{p}(0) = 0$ (in first approximation when acoustic radiation is neglected) and the closed end (supposed to be a perfectly rigid wall) at $x = L$ corresponds to an acoustic volume velocity $\widetilde{u}(L) = 0$. Reporting this two boundary conditions into Eq. (8) gives

$$\begin{cases} \widetilde{p}(L) = T_{pu}\widetilde{u}(0) \\ 0 \quad = T_{uu}\widetilde{u}(0) \end{cases}. \tag{10}$$

This equation has a non-trivial solution ($\widetilde{u}(0) \neq 0$) only if

$$T_{uu} = 0, \tag{11}$$

which defines the onset condition of an open-closed standing-wave engine.
Actually, the coefficients of the transfer matrix are complex quantities which depend on the frequency and the hot temperature[1] T_H on the right side of the stack (Fig. 1). This means that solving Eq. (11) is equivalent to solving a system of two equations with two unknown variables

$$\begin{cases} \Re(T_{uu}(\omega, T_H)) = 0 \\ \Im(T_{uu}(\omega, T_H)) = 0 \end{cases}, \tag{12}$$

where $\Re(T_{uu})$ (resp. $\Im(T_{uu})$) is the real part (resp. imaginary part) of T_{uu}. The solution of this system is the couple $(\omega_{onset}, T_{H,onset})$ including the onset angular frequency and the hot temperature (on the right side of the stack) which is necessary for the amplification of thermoacoustic instability in the engine.

1.2 Expansion of the theory for more complicated geometries

The use of the transfer matrix formalism allows to derive the onset conditions for a large number of engines of different geometries.
For instance, it is quite direct from the results presented in Sec. 1.1 to derive the onset conditions for other kinds of standing-wave engines, by simply changing the boundary conditions at both ends of the waveguide shown in Fig. 1. The onset conditions for the three other configurations are then formulated as :

$$T_{pp} = 0 \quad \text{for a "closed-open" engine,} \tag{13}$$
$$T_{pu} = 0 \quad \text{for a "open-open" engine,} \tag{14}$$
$$T_{up} = 0 \quad \text{for a "closed-closed" engine.} \tag{15}$$

But it is also quite direct to derive the onset conditions for other thermoacoustic engines, as it will be discussed below.

Coupling with an alternator The coupling between the acoustic resonator and an electrodynamic alternator, for example at the end $x = 0$ as it is shown in Fig. 2-(a), can also be described by an impedance condition $\widetilde{Z}(0) = \widetilde{Z}_{alt}$, where

$$\widetilde{Z}_{alt} = R_{ma} + \frac{i}{\omega C_{ma}} - i\omega M_{ma} \tag{16}$$

is the equivalent impedance of the electrodynamic alternator. R_{ma} is the acoustic resistance equivalent to the mechanical losses, C_{ma} is the acoustic compliance equivalent to the compliance of the suspensions and M_{ma} is the acoustic mass equivalent to the moving mass of the alternator. Then, the onset condition of the straight engine coupled with an alternator at $x = 0$ (see Fig. 2-(a)) can be written as

$$T_{up} + \frac{T_{uu}}{\widetilde{Z}_{alt}} = 0. \tag{17}$$

Closed-loop thermoacoustic engine The transfer matrix formalism also allows to define the onset conditions of a closed-loop traveling-wave engine (Fig. 2-(b)). In this case, equation (8) is still valid if the propagation of a plane wave in the

[1] In first approximation, when a linear temperature distribution is assumed. Actually, the coefficients also depend on the spatial distribution of the temperature field along the thermoacoustic core.

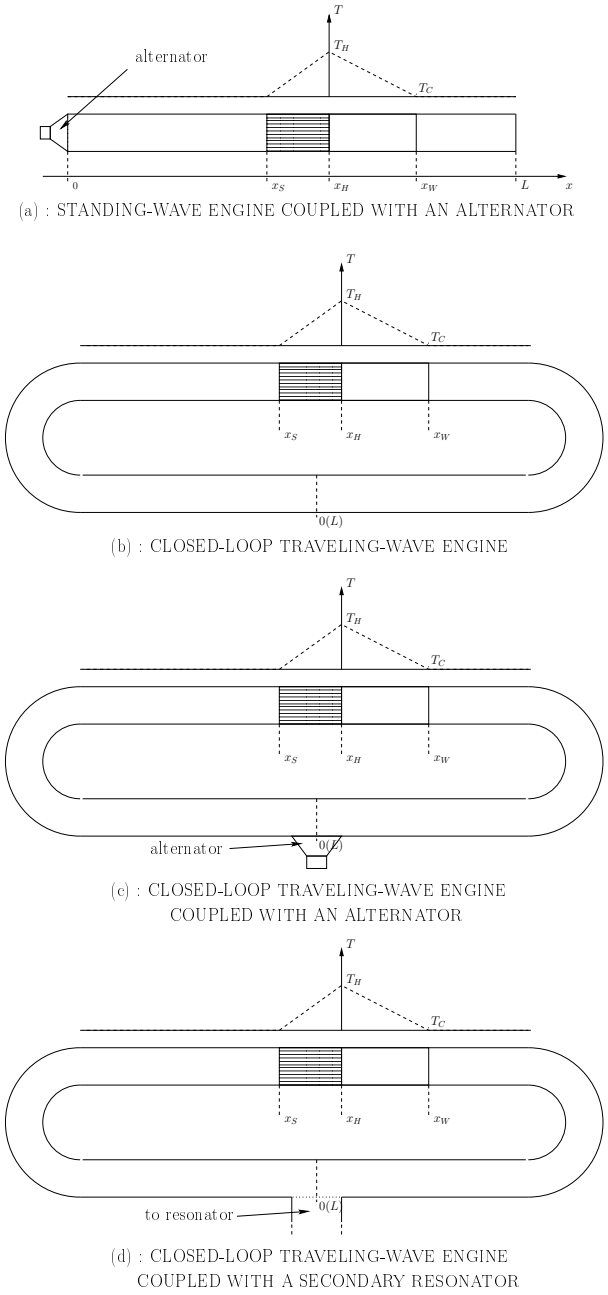

FIGURE 2. DRAWING OF DIFFERENT GEOMETRIES OF THERMOACOUSTIC-WAVE GENERATORS.

closed loop is supposed to be equivalent to the propagation in a straight duct with the same unwrapped length (the effects due to the loop curvature are assumed to be negligible). Then, the continuity equations for the acoustic pressure and volume velocity at position $x = 0$ allows to rewrite Eq. (8) as

$$\begin{pmatrix} \widetilde{p}(0) \\ \widetilde{u}(0) \end{pmatrix} = \begin{pmatrix} T_{pp} & T_{pu} \\ T_{up} & T_{uu} \end{pmatrix} \times \begin{pmatrix} \widetilde{p}(0) \\ \widetilde{u}(0) \end{pmatrix}. \tag{18}$$

This equation has a non-zero solution only if the determinant of the matrix $(T_{tot} - I_2)$ is equal to zero[2]. The onset condition of the closed-loop engine is thus given by

$$(T_{pp} - 1)(T_{uu} - 1) - T_{up}T_{pu} = 0. \tag{19}$$

Finally, as for a standing-wave engine, the coupling between the closed-loop resonator and an alternator [10] or a secondary resonator (as a 1/4-wavelength resonator [7]), as illustrated in Figs. 2-(c) and 2-(d), can be described by adding an impedance condition at position $x = 0$ and an expression of the onset condition can be developped in an equivalent form.

In summary, it is possible to have a complete analytical description of the onset conditions for a large number of thermoacoustic engines of different geometries. However, it is worth noting that the analytical expressions of the matrices T_s and T_w representing the propagation in the thermoacoustic core can only be approximative, due to the assumptions concerning the geometry of the stack or the shape of the temperature field. Moreover, this theoretical approach takes no account of the geometry or efficiency of the heat exchangers situated at x_s, x_H et x_w and which are used to establish the thermal gradient along the thermoacoustic core.

A new approach is thus proposed, in which the thermoacoustic core is considered as a "black box" (with unknown geometrical and thermophysical properties) characterized by means of an experimental setup presented in the next section.

2 MEASUREMENT OF THE TRANSFER MATRIX OF A THERMOACOUSTIC CORE

2.1 Experimental setup

A schematic drawing of the experimental apparatus is shown in Fig. 3. It is made up of the thermoacoustic core under study, located between x_s and x_w and inserted between two straight PVC ducts of length $L = 2m$ and inner radius $R = 16,45mm$. The left duct is connected with an electrodynamic loudspeaker generating a swept sine signal from 50 to $200Hz$. The end of the right duct is either kept open, or closed with a rigid wall. Two pairs of microphones are flush mounted along each duct at both sides of the thermoacoustic core (see Fig. 3). In order to prevent from large measurement errors, vacuum grease is used for airtightness at the locations where ducts, thermoacoustic core and microphones are connected each other. The microphone separation Δx is chosen

[2] I_2 is the identity matrix 2×2.

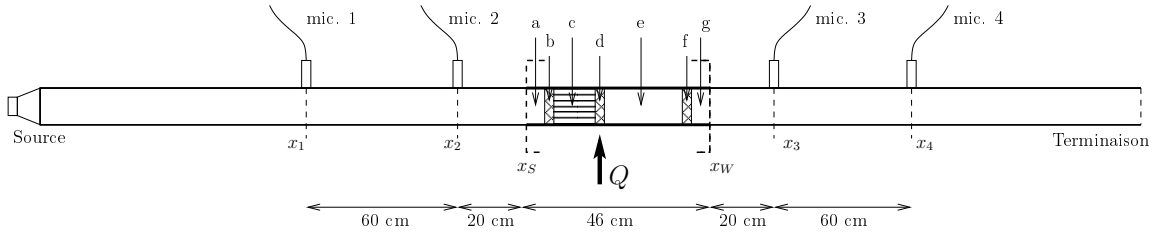

FIGURE 3. DRAWING OF THE EXPERIMENTAL APPARATUS USED FOR MEASUREMENTS OF THE TRANSFER MATRIX OF THE CORE.

in order to minimize errors in the transfer functions estimate, according to the criterium given by Àbom [1]

$$0,1\pi < k_0\Delta x < 0,8\pi. \tag{20}$$

The microphone separation $\Delta x = 60cm$ used for the apparatus seems to be the most appropriate to make measurements on the frequency range $[50,200]Hz$.
The studied thermoacoustic core is a stainless steel waveguide of inner radius $R_w = 16,7mm$ and length $l = 46cm$. It is made up of a first duct section (Fig3-a), a cold heat exchanger (b), a ceramic sample (stack) of length $l_s = 7,2cm$ (c), a hot heat exchanger (d), a duct section (e) called the passive part, a second cold heat exchanger (f), and a final duct section (g). The open pores of the stack have square boundaries of semi-width $R_s = 0,6mm$. The cold heat exchangers are made up of two copper pipes passing through a honeycombed aluminium disk, with flowing water inside the pipes at room temperature. The hot heat exchanger is made up of a piece of ceramic sample (the same porous medium used for the stack) in which a Nichrome resistance wire is coiled. The thickness of the sample is $1cm$ and the heat resistance wire is connected to an electrical DC power supply controling the heat Q_H dissipated by Joule effect into the wire.
The measurement method used here is a four-microphone method. A short review of the theory of this method is presented in the next section. For more details, see for instance Refs. [1,4].

2.2 Four-microphone method

Considering the apparatus shown in Fig. 3, the acoustic pressure in duct comprised between $x = 0$ and $x = x_s$ can be separated into two counterpropagating plane waves, so that the complex amplitude of the acoustic pressure is written as

$$\begin{aligned}\widetilde{p}(x) &= \widetilde{p}^{+}(x) + \widetilde{p}^{-}(x) \\ &= \widetilde{p}^{+}(x_s)e^{jk_w(x-x_s)} + \widetilde{p}^{-}(x_s)e^{-jk_w(x-x_s)} \quad \forall x \in [0,x_s],\end{aligned} \tag{21}$$

where x_s is the coordinate of the left end of the thermoacoustic core.

In the same way, the pressure in duct comprised between $x = x_w$ and $x = L$ is given by

$$\widetilde{p}(x) = \widetilde{p}^{+}(x_w)e^{jk_w(x-x_w)} + \widetilde{p}^{-}(x_w)e^{-jk_w(x-x_w)} \quad \forall x \in [x_w,L], \tag{22}$$

where x_w is the coordinate of the right end of the thermoacoustic core. From Eq. (21) and Eq. (22), the four counterpropagating components of acoustic pressures on both sides of the thermoacoustic core can be expressed as functions of the acoustic pressures $\widetilde{p}_1 = \widetilde{p}(x_1)$, $\widetilde{p}_2 = \widetilde{p}(x_2)$, $\widetilde{p}_3 = \widetilde{p}(x_3)$ and $\widetilde{p}_4 = \widetilde{p}(x_4)$ at the location of each microphone :

$$\widetilde{p}^{+}(x_s) = \frac{\widetilde{p}_2 e^{jk_w(x_s-x_1)} - \widetilde{p}_1 e^{jk_w(x_s-x_2)}}{2j\sin[k_w(x_2-x_1)]}, \tag{23}$$

$$\widetilde{p}^{-}(x_s) = \frac{\widetilde{p}_1 e^{-jk_w(x_s-x_2)} - \widetilde{p}_2 e^{-jk_w(x_s-x_1)}}{2j\sin[k_w(x_2-x_1)]}, \tag{24}$$

$$\widetilde{p}^{+}(x_w) = \frac{\widetilde{p}_4 e^{-jk_w(x_3-x_w)} - \widetilde{p}_3 e^{-jk_w(x_4-x_w)}}{2j\sin[k_w(x_4-x_3)]}, \tag{25}$$

$$\widetilde{p}^{-}(x_w) = \frac{\widetilde{p}_3 e^{jk_w(x_4-x_w)} - \widetilde{p}_4 e^{jk_w(x_3-x_w)}}{2j\sin[k_w(x_4-x_3)]}, \tag{26}$$

Thus measuring the pressure (modulus and phase) from each microphone allows to estimate $\widetilde{p}^{\pm}(x_s)$ and $\widetilde{p}^{\pm}(x_w)$, and then to deduce either the scattering matrix of the thermoacoustic core

$$\begin{pmatrix}\widetilde{p}^{+}(x_w)\\ \widetilde{p}^{-}(x_s)\end{pmatrix} = \begin{pmatrix}T^{+} & R^{-}\\ R^{+} & T^{-}\end{pmatrix} \times \begin{pmatrix}\widetilde{p}^{+}(x_s)\\ \widetilde{p}^{-}(x_w)\end{pmatrix}, \tag{27}$$

or its transfer matrix

$$\begin{pmatrix}\widetilde{p}(x_w)\\ \widetilde{u}(x_w)\end{pmatrix} = \begin{pmatrix}T_{pp} & T_{pu}\\ T_{up} & T_{uu}\end{pmatrix} \times \begin{pmatrix}\widetilde{p}(x_s)\\ \widetilde{u}(x_s)\end{pmatrix}, \tag{28}$$

where the volume velocity $\widetilde{u}$ is given by

$$\widetilde{u}(x) = \frac{(1-f_v)}{j\omega\rho_0}\left(\frac{\partial\widetilde{p}}{\partial x}\right) = \frac{1}{Z_c}[\widetilde{p}^{+}(x) - \widetilde{p}^{-}(x)], \tag{29}$$

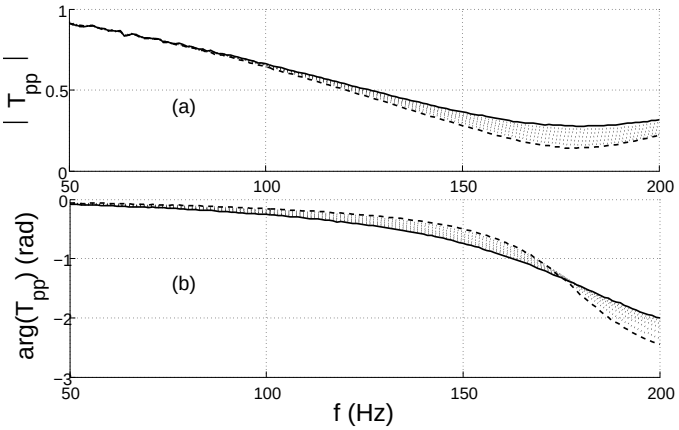

FIGURE 4. EVOLUTION OF THE EXPERIMENTAL COEFFICIENT T_{pp} OF THE TRANSFER MATRIX OF THE CORE AS A FUNCTION OF THE FREQUENCY AND FOR SEVERAL INCREMENTS OF HEAT, IN MAGNITUDE (a) AND IN PHASE (b). $--$: $Q_{min} = 7,8W$, — : $Q_{max} = 83W$, $\cdots$: INTERMEDIATE Q_i.

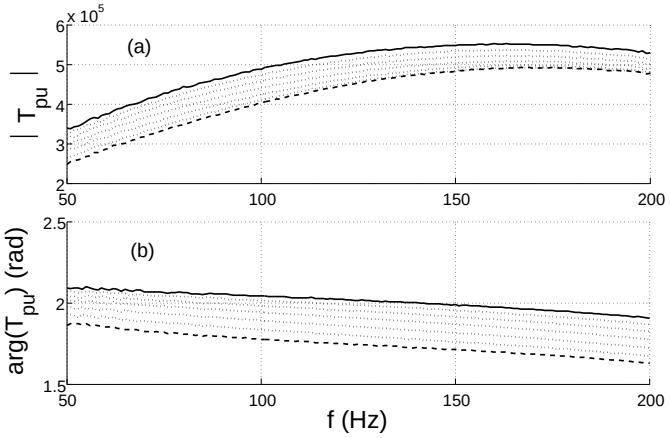

FIGURE 5. EVOLUTION OF THE EXPERIMENTAL COEFFICIENT T_{pu} OF THE TRANSFER MATRIX OF THE CORE AS A FUNCTION OF THE FREQUENCY AND FOR SEVERAL INCREMENTS OF HEAT, IN MAGNITUDE (a) AND IN PHASE (b). $--$: $Q_{min} = 7,8W$, — : $Q_{max} = 83W$, $\cdots$: INTERMEDIATE Q_i.

with $Z_c = \frac{Z_w k_0}{k_w}$.
However, it clearly appears that Eq. (28) is a system of two equations with four unknown variables (the four matrix coefficients). That is the reason why it is necessary to make two measurements with two different configurations of the experimental setup [4]. The "two-loads" method used here consists in making one measurement with a first acoustic load at the right end of the duct (see Fig. 3), and then a second measurement with a different acoustic load. In the work presented here, the two acoustic loads at the end of the duct are the open duct and the duct closed by a rigid wall, respectively.
It is important to note that in spite of the simplicity of the implementation of this experimental setup, it is a strongly indirect method and each measurement error can impact significantly the final results. It is thus wise to bring all the necessary precautions during the measurements (concerning for instance the signal processing or the relative calibrations of the microphones).

2.3 Theoretical and experimental results

In this section, theoretical and experimental coefficients of the transfer matrix are compared. However, it is important to note that this comparison is only qualitative because it is difficult to get a direct relation between the hot temperature T_H used in the analytical description and the heat supply Q_H actually dissipated in the heating wire. The theoretical transfer matrix of the thermoacoustic core is calculated for a given temperature T_H at the location of the hot heat exchanger and using an exponential profile for the temperature field. In experiments, the temperature T_H is not measured and the transfer matrix is measured for various heating power supplies Q_H.
During the measurements, the temperature at the location of the cold heat exchangers is assumed to be constant and equal to the room temperature $T_C = 294K(21°C)$.
The Figures 4 and 5 show the experimental results for the modulus (a) and phase (b) of the coefficients T_{pp} and T_{pu} of the transfer matrix, as functions of the frequency and for several increments of heating power supply Q_H. It appears that these results are qualitatively in good accordance with the results from theoretical calculations of T_{pp} and T_{pu} shown in Figs. 6 and 7. In addition to the fact that the heat supplies Q_H (Figs 4 and 5) do not directly correspond with the hot temperatures T_H (Figs 6 and 7), some discrepancy between the experimental and theoretical results can be partly explained by the presence of some elements which are not taken into account in the theoretical model, like the presence of the heat exchangers for instance.
The results obtained for the other coefficients of the transfer matrix or those of the scattering matrix are not exposed here, but the conclusions are the same.

3 PREDICTION OF THE ONSET CONDITIONS FROM THE MEASURED TRANSFER MATRIX

Once the transfer matrix of the thermoacoustic core is measured on the frequency range $[50,200]Hz$ for several increments of heat Q_H, the analytical expressions of the matrices T_s and T_w are replaced with the experimental data in the model described in

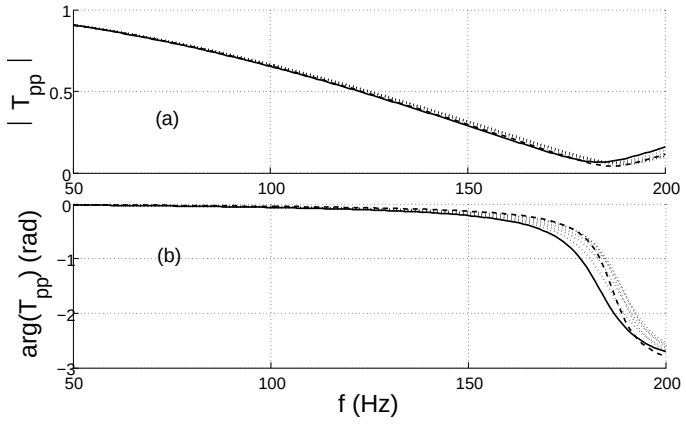

FIGURE 6. EVOLUTION OF THE THEORETICAL COEFFICIENT T_{pp} OF THE TRANSFER MATRIX OF THE CORE AS A FUNCTION OF THE FREQUENCY AND FOR SEVERAL HOT TEMPERATURES, IN MAGNITUDE (a) AND IN PHASE (b). $--$: $T_{H,min} = T_C + 50K$, — : $T_{H,max} = T_C + 250K$, $\cdots$: INTERMEDIATE T_H.

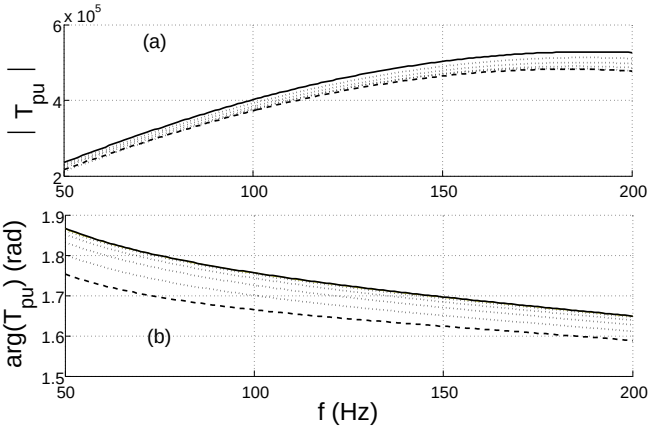

FIGURE 7. EVOLUTION OF THE THEORETICAL COEFFICIENT T_{pu} OF THE TRANSFER MATRIX OF THE CORE AS A FUNCTION OF THE FREQUENCY AND FOR SEVERAL HOT TEMPERATURES, IN MAGNITUDE (a) AND IN PHASE (b). $--$: $T_{H,min} = T_C + 50K$, — : $T_{H,max} = T_C + 250K$, $\cdots$: INTERMEDIATE T_H.

Sect. 1.1. It is then possible to predict from this model the heating power supply Q_{onset} which must be reached for the onset of the thermoacoustic instability (together with the corresponding frequency f_{onset}) in a thermoacoustic engine of specified geometry.
In order to compare the predictions of the model with actual onset conditions, this method is applied to a straight "open-closed" standing-wave engine (see Fig. 1). The thermoacoustic core characterized beforehand is now connected to two straight cylindrical PVC ducts of lengths L_1 (for the tube on the right side) and L_2 (for the tube on the left side). For the study presented in this work, the tube on the left side is closed and its length is kept constant at $L_2 = 10cm$. The other tube is open to free space and its length L_1 is varied from $17cm$ to $1m$.
The onset conditions, i.e. the onset frequency f_{onset} and the onset heating power supply Q_{onset}, of the "open-closed" standing-wave generator as functions of the length L_1 are shown in Figs. 8-(a) and 8-(b). The predictions of the model are very close to the onset conditions observed in experiments, and in spite of a gap of a few Hertz for the frequency, it is worth noting that the evolution of (f_{onset}, Q_{onset}) as a function of L_1 is well reproduced by the model.

However the results obtained from this semi-analytical approach cannot be considered as completely satisfying for the moment : some problems have to be troubleshooted in the solving of Eq. (12). Indeed, it seems to be impossible to find a single angular frequency ω which allows to cancel both the real part and the imaginary part of the coefficient T_{uu}. In fact, the solving of Eq. (12) gives two frequency ω_1 and ω_2 defined by

$$\begin{cases} \Re(T_{uu}(\omega_1, Q_i)) = 0 \\ \Im(T_{uu}(\omega_2, Q_i)) = 0 \end{cases}, \tag{30}$$

and it appears that the onset does not exactly correspond to $\omega_1 = \omega_2$ for $Q_i = Q_{onset}$.
To find estimations in good agreement with experiments, it is thus necessary to fix a criterium df on the frequency such that the onset power Q_{onset} is reached when

$$|\omega_2 - \omega_1| \leq 2\pi df, \tag{31}$$

and the onset angular frequency ω_{onset} is then simply evaluated by

$$\omega_{onset} = \frac{1}{2}(\omega_1 + \omega_2). \tag{32}$$

The results shown in Fig. 8 are obtained for $df = 14Hz$.
In addition, the small differences observed in Fig. 8-(b) between the experimental onset frequency and the predicted onset frequency can be explained by other reasons. Firstly, the radiation impedance at the location of the open pipe is not taken into account in the model. Secondly, the measurement of the transfer

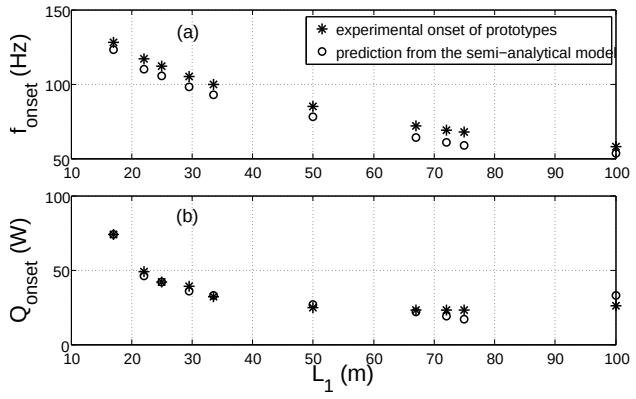

FIGURE 8. ONSET CONDITIONS OF A STRAIGHT "OPEN-CLOSED" STANDING-WAVE THERMOACOUSTIC GENERATOR AS FUNCTIONS OF THE LENGTH L_1 : f_{onset} (a) AND Q_{onset} (b). THE PREDICTIONS FROM THE SEMI-ANALYTICAL MODEL ($\circ$) ARE COMPARED WITH REAL ONSET CONDITIONS OF PROTOTYPES ($*$).

matrix of the thermoacoustic core and the measurement of actual onset conditions of the standing-wave engine were not made with the exactly same room temperatures ($T_C = 21°C$ in the first experiment and $T_C = 23,2°C$ in the second one).
The semi-analytical model is able to predict the onset conditions of a standing-wave engine which are close to those observed in experiments, but the necessity to define a criterium in order to fit the theoretical results with the experimental ones still represents a serious trouble in the model which must be solved. New approaches are currently in hand to formulate the onset conditions properly. More precisely, works are now in progress in order to derive the onset conditions from the measured scattering matrix (instead of the transfer matrix) and from the computation of a complex frequency $\omega = \Omega + j\alpha$, for which the sign of its imaginary part α indicates if sound waves are amplified or attenuated.

4 CONCLUSION

The use of a formalism based on the transfer matrices makes possible to express the onset conditions of the thermoacoustic instability for a large number of engines of various geometries. However, the theory requires to know the analytical expressions of the transfer matrix of the thermoacoustic core. Approximative expressions can be obtained when the stack is made of parallel plates or straight duct pores, and with some assumptions concerning in particular the shape of the temperature field [2,3,8,9]. But when the stack is replaced by a regenerator made up of a random stacking of metal wire mesh and when the shape of the temperature field along the core is poorly known, the theoretical modeling of the acoustic propagation inside the thermoacoustic core becomes difficult to carry out. That is the reason why an experimental approach of the problem is proposed, which could, once the results introduced into a model, predict the onset of a thermoacoustic engine without strong assumptions concerning the thermoacoustic core.
By using a four-microphone method, it is possible to measure the transfer matrix of the thermoacoustic core in function of the heat power supply Q_H. These results are then introduced into an appropriate model to predict the onset conditions of a thermoacoustic engine. For a straight standing-wave generator, the model is able to predict the onset conditions with good accuracy, but it also appears some troubles in the solving due to the theoretical formulation. Work is currently in hand in order to develop a more appropriate formulation and also to judge potential of this new approach to properly predict the onset conditions of various types of thermoacoustic-wave generators.

ACKNOWLEDGMENT

The authors would like to thank Jean-Pierre Dalmont, professor in the Laboratoire d'Acoustique de l'Université du Maine, for his advices concerning the setting up of the experimental apparatus.

NOMENCLATURE

c_0 Adiabatic sound velocity ($m.s^{-1}$)
C_{ma} Acoustic compliance ($m.N^{-1}$)
f_κ Thermal function
f_ν Viscous function
I_2 Identity matrix 2×2
j $\sqrt{-1}$
k_0 Wave number (m^{-1})
k_w Complex wave number (m^{-1})
l Length (m)
L Length (m)
M_{ma} Acoustic mass (kg)
p Acoustic pressure in the time domain (Pa)
$\widetilde{p}$ Complex amplitude of the acoustic pressure in the frequency domain (Pa)
Q_H Heating power supply (W)
R Radius (m)
R_{ma} Acoustic resistance ($N.s.m^{-1}$)
S_w Tube cross section (m^2)
t Time variable (s)
T Transfer matrix
T_C Temperature at the cold heat exchanger - Room temperature (K)
T_H Temperature at the hot heat exchanger (K)
u Volume velocity in the time domain ($m.s^{-1}$)

$\widetilde{u}$ Complex amplitude of the volume velocity in the frequency domain ($m.s^{-1}$)
x Spatial variable (m)
$\widetilde{Z}$ Impedance
α Imaginary part of a complex angular frequency (s^{-1})
γ Specific heat ratio
ρ_0 Density of fluid ($kg.m^{-3}$)
ω Angular frequency (s^{-1})
Ω Real part of a complex angular frequency (s^{-1})
$\Im$ Imaginary part of a complex number
$\Re$ Real part of a complex number

REFERENCES

[1] Boden H., Abom M., "Influence of errors on the two-microphone method for measuring acoustic properties in ducts", *J. Acoust. Soc. Am.* 79 (2), 541-549 (1986)

[2] Roh H.S., Arnott W.P., Sabatier J.M., Raspet R., "Measurement and calculation of acoustic propagation constants in arrays of small air-filled rectangular tubes", *J. Acoust. Soc. Am.* 89 (6), 2617-2624 (1991)

[3] Arnott W.P., Bass H.E., Raspet R., "General formulation of thermoacoustics for stacks having arbitrarily shaped pore cross sections", *J. Acoust. Soc. Am.* 90 (6), 3228-3237 (1991)

[4] Ajello G., "Mesures acoustiques dans les guides d'ondes en présence d'écoulement : Mise au point d'un banc de mesure - application à des discontinuités", PhD. Thesis, Université du Maine, 1997

[5] Watanabe M., Prosperetti A., Yuan H., "A simplified model for linear and nonlinear processes in thermoacoustic prime movers. Part 1. Model and linear theory", *J. Acoust. Soc. Am.* 102 (6), 3484-3496 (1997)

[6] Karpov S., Prosperetti A. "Linear thermoacoustic instability in the time domain", *J. Acoust. Soc. Am.* 103 (6), 3309-3317 (1998)

[7] Backhaus S., Swift G.W., "A thermoacoustic-Stirling heat engine : Detailed study", *J. Acoust. Soc. Am.* 107 (6), 3148-3166 (2000)

[8] Job S., "Etudes théoriques et expérimentales d'un générateur thermoacoustique annulaire à ondes progressives", PhD. Thesis, Université du Maine, 2001

[9] Penelet G., "Etude expérimentale et théorique des processus non linéaires de saturation dans un générateur d'ondes thermoacoustique annulaire", PhD. Thesis, Université du Maine, 2004

[10] Backhaus S., Tward E., Petach M., "Traveling-wave thermoacoustic electric generator", *Appl. Phys. Lett.* 85 (6), 1085-1087 (2004)

[11] Penelet G., Job S., Gusev V., Lotton P., Bruneau M., "Dependence of sound amplification on temperature distribution in annular thermoacoustic engines", *Acustica Acta Acustica* 88, 986-997 (2005)